PB82-143371

Predicting Pressure Loss for Pulse Jet Filters

GCA Corp.
Bedford, MA

Prepared for

Industrial Environmental Research Lab.
Research Triangle Park, NC

1981

U.S. Department of Commerce
National Technical Information Service
NTIS.

TECHNICAL REPORT DATA
(Please read Instructions on the reverse before completing)

1. REPORT NO. EPA-600/J-81-406	2. Journal Article	3. RI PB82-143371
4. TITLE AND SUBTITLE Predicting Pressure Loss for Pulse Jet Filters*		5. REPORT DATE October 1981 6. PERFORMING ORGANIZATION CODE 2362014
7. AUTHOR(S) Richard Dennis (GCA, Bedford, MA 01730)/John E. Wilder (S.D. Warren, Westbrook, ME 04092)/Dale L. Harmon (EPA/IERL-RTP)		8. PERFORMING ORGANIZATION REPORT NO.
9. PERFORMING ORGANIZATION NAME AND ADDRESS GCA/Technology Division Bedford, MA 01730		10. PROGRAM ELEMENT NO. 11. CONTRACT/GRANT NO.
12. SPONSORING AGENCY NAME AND ADDRESS **EPA, Office of Research and Development Industrial Environmental Research Laboratory Research Triangle Park, NC 27711**		13. TYPE OF REPORT AND PERIOD COVERED Journal Article; 1981 14. SPONSORING AGENCY CODE **EPA/600/13**

15. SUPPLEMENTARY NOTES *Cleared May 1980 as "The Mechanics of Pulse Jet Filtration." Published in the Journal of the Air Pollution Control Association, Vol. 31, No. 9, pp 987-992, September 1981.

16. ABSTRACT

The paper discusses the prediction of pressure loss for pulse jet filters. The analysis of pressure loss characteristics for the filters suggests that the relationship between dust adhesion to the fabric and the opposing force generated by pulse jet action plays a major role in dust removal. Hence, fabric cleanability is examined in terms of the adhesion/cohesion forces bonding the dust to the fabric vs. the intensity and frequency of the dust dislogement forces produced by the high energy air pulses. The effect of jet size and location, jet air volume, and the intensity (pressure) and duration of the jet pulses is related to operating pressure loss. The mechanics of energy transfer from the jet pulse to the dust-laden fabric are explored in terms of jet pressure, solenoid valve action, the ratio of delivered pulse air volume to bag (tube) volume, and the elastic and flex properties of the felt bags. Effective and actual fabric dust holdings before and after cleaning are discussed with respect to steady-state dust deposition and removal rates, and operating pressure losses. Finally, predictive equations are proposed for estimating pressure loss over a broad range of design and operating parameters.

17. KEY WORDS AND DOCUMENT ANALYSIS

a. DESCRIPTORS	b. IDENTIFIERS/OPEN ENDED TERMS	c. COSATI Field/Group
Pollution Dust Jets Air Cleaners Filtration Fabrics Pressure Reduction Predictions	Pollution Control Stationary Sources Pulse Jet Filters Fabric Filters	13B 11G 20D 13A, 13I 07D 11E 14G

18. DISTRIBUTION STATEMENT **Release to Public**	19. SECURITY CLASS *(This Report)* **Unclassified**	21. NO. OF PAGES 6
	20. SECURITY CLASS *(This page)* **Unclassified**	22. PRICE

EPA Form 2220-1 (9-73)

REPRODUCED BY
NATIONAL TECHNICAL
INFORMATION SERVICE
U.S. DEPARTMENT OF COMMERCE
SPRINGFIELD, VA 22161

EPA-600/J-81-406
Journal Article

Predicting Pressure Loss for Pulse Jet Filters

Richard Dennis
GCA/Technology Division
Bedford, Massachusetts

John E. Wilder
S. D. Warren, A Division of Scott Paper Company
Westbrook, Maine

Dale L. Harmon
U.S. Environmental Protection Agency
Research Triangle Park, North Carolina

The analysis of pressure loss characteristics for pulse jet filters suggests that the relationship between dust adhesion to the fabric and the opposing force generated by pulse jet action plays a major role in dust removal. Hence, fabric cleanability is examined in terms of the adhesion-cohesion forces bonding the dust to the fabric vs. the intensity and frequency of the dust dislodgement forces produced by the high energy air pulses. The effect of jet size and location, jet air volume, and the intensity (pressure) and duration of the jet pulses is related to operating pressure loss.

The mechanics of energy transfer from the jet pulse to the dust-laden fabric are explored in terms of jet pressure, solenoid valve action, the ratio of delivered pulse air volume to bag (tube) volume, and the elastic and flex properties of the felt bags. Effective and actual fabric dust holdings before and after cleaning are discussed with respect to steady-state dust deposition and removal rates, and operating pressure losses. Finally, predictive equations are proposed for estimating pressure loss over a broad range of design and operating parameters.

Background Studies

Despite widespread applications, the actual physical processes determining the performance of pulse jet filters are not clearly understood and sometimes incorrectly defined. The investigations of Dennis and Silverman,[1] Dennis and Wilder,[2] Leith, First, and Feldman,[3] Ellenbecker and Leith,[4,5] Bakke,[6] and Lefkowitz[7] encompass much of the basic research. Although these studies help to explain how pulse jet filters work, none provide a clear insight as to the actual physical processes taking place during filtration or fabric cleaning. Recently, Dennis and Klemm[8] have proposed that the filter drag, S, for a single bag pulse jet unit can be described by the relationship:

$$S = S_E + (K_2)_c W_c + K_2 \Delta W \qquad (1)$$

where S_E is the residual drag for the used felt with its residual dust loading; $(K_2)_c$, the specific resistance coefficient for the cycling fraction of the total dust loading that is alternately dislodged and redeposited on the fabric; W_c, the cycling portion of the dislodgeable dust holding;[8] and K_2, the specific resistance coefficient for the freshly deposited dust fraction, ΔW, that accumulates over the filtration interval, Δt, at inlet concentration, C, and face velocity, V. Despite the large amounts of dust residing upon or within felt fabrics, ~400 to 1000 g/m^2, various investigators have determined that less than 1 to 10% of the dust dislodged by the cleaning action actually descends to the dust hopper.[5,8] The very brief duration of a typical cleaning pulse, ~0.1 s, does not permit significant gravitational fallout in contrast to that obtained with mechanically shaken baghouses in which the gas flow is interrupted for as much as 2 to 5 minutes.

There is general agreement that dust dislodgement occurs when the separating force, F_s, associated with the jet pulse exceeds the adhesive force, F_A, binding the dust to the fabric.[5,8] Dennis and Klemm have postulated, however, that the surface dust loading prior to cleaning, $W_c + \Delta W$, is uniquely defined by the adhesive force between the dust layer and fabric, F_A, and the separation force, F_S, produced by the average acceleration imparted to the dust layer by the jet pulse.[8] Furthermore, they have asserted, based upon prior studies,[2] that the magnitude of W_c depends mainly upon the F_A-F_S relationship for the *specific dust-fabric combination* with large variations in inlet concentration and filtration velocity exerting little effect on W_c values. It was also reported that the specific resistance coefficient, $(K_2)_c$, for the cycling dust loading, W_c, should be considerably lower than that for the freshly deposited dust, ΔW, because of the highly agglomerated state of the cycling layer.[8] Additionally, whereas W_c was described as varying from 400 to 1000 g/m^2, ΔW levels usually ranged from only 3 to 60 g/m^2.[5,8] Although Eq. (1) appears to offer a convenient method for drag estimation, it cannot be applied directly without definition of the $(K_2)_c$ and W_c terms. Therefore, Dennis and Klemm proposed the following restructuring:

$$P = (P_E)_{\Delta W} + CK_2V^2\Delta t \qquad (2)$$

in which filter pressure loss, P, is expressed in pressure rather than drag units and the fabric loading, ΔW, deposited during

the filtration interval, Δt, is expressed as $CV\Delta t$. The variable, $(P_E)_{\Delta W}$, herein defined as the *effective residual pressure loss*, and containing the terms P_E and $(K_2)_c W_c V$, corresponds to the intercept of the linear extrapolation of the pressure-time trace on the pressure axis at the resumption of filtration.

For the experimental pressure curves shown in Figure 1 denoting coal fly ash filtration on needled Dacron felt, the effective residual pressure was related to the compressed air pressure as shown below:

$$(P_E)_{\Delta W} = \alpha P_j^{-\beta} \qquad (3)$$

Nomenclature

Symbol	Description	Unit(s)
A	Bag area, system	m^2
A_j	Jet nozzle cross section	m^2
a_i	Bag area, ith surface area increment	m^2
a_{max}	Peak bag deceleration	m/s^2
$\bar{a}$	Fabric and dust acceleration	m/s^2
C	Inlet dust concentration	g/m^3
F_A	Adhesive force/unit area	N/m^2
F_s	Separating force/unit area	N/m^2
G	Bag elongation parameter	$cm^2\text{-}s^2/g$
g	Dust mass (grams)	g
g_a	Gravity acceleration	g cm/s^2 (or g)
K_2	Specific resistance coefficient	N-min/g-m
$(K_2)c$	Specific resistance coefficient cycled dust loading	N-min/g-m
k	Constant in Eq 14	2.12
M	Jet air, mass flow rate	g/s
M_e	Bag flexing parameter	$cm^2\text{-}s^2/g$
MMD_a	Mass media diameter, actual	μm
n_b	Number of bags	kPa
P	Filter pressure loss	kPa
P_b	Bag static pressure before pulsing	kPa
$(PE)_{\Delta W}$	Filter pressure loss (effective) before filtration	kPa
P_j	Pulse jet reservoir pressure, gauge	kPa
P_{ja}	Pulse jet reservoir pressure, absolute	kPa
P_{max}	Maximum pressure clean side of bag	kPa
r	Bag radial displacement	cm
r_{max}	Maximum bag displacement	cm
S	Filter drag	$N\text{-}min/m^3$
S_E	Filter drag, effective residual	$N\text{-}min/m^3$
S_i	Filter drag, ith surface area increment	$N\text{-}min/m^3$
$\bar{S}$	Filter drag, system average	$N\text{-}min/m^3$
T_{ja}	Absolute temperature, compressed air	°K
t_s	Solenoid valve opening time	s
Δt	Time, filtration interval	min
V	Filtration (face) velocity	m/min
V_b	Bag volume	m^3
V_{max}	Maximum radial velocity	cm/s
V_p	Primary jet air volume	m^3
V_s	Secondary jet air volume	m^3
W	Fabric dust loading	g/m^2
W_c	Fabric dust loading, cycling	g/m^2
ΔW	Dust loading added during filtration interval	g/m^2
α	Constant	Dimensionless
β	Constant	Dimensionless
ρ	Bag and dust mass per unit area	g/m^2
ρ_b	Ambient (bag) air density	kg/m^3
σ_g	Geometric standard deviation	Dimensionless
σ_{max}	Bag stopping force per unit area	$g/cm\text{-}s^2$

where α and β are constants whose values depend upon the type of pulse, direct or damped,* and P_j is the compressed air pressure. Eq. (2) and (3) constitute useful guidelines for predicting fabric pressure loss for a specific dust-fabric combination, provided that the pulse jet nozzle configuration (including jet diameter and location) and bag dimensions remain unchanged.

The research described in this paper offers an added dimension to the limited predictive capabilities of Eq. (2) and (3) by allowing for variability in (a) compressed air nozzle size, (b) operating mode of jet systems, and (c) bag size and physical properties.

Dynamics of Bag Motion

Fabric Acceleration—Deceleration Forces

Prior analyses have suggested that a unit separation force of roughly 500 N/m^2 is required for the complete dislodgement of a coal fly ash surface layer from a Dacron felt.[8] Laboratory observations have also indicated that the dislodgement of dust from felt fabrics, as well as that from woven glass and cotton, is usually characterized by detachment at the dust layer–fabric interface where the adhesive bonds are weakest.[2,8] It is recognized that abnormal electrical charge factors, condensation, chemical reactions and/or very fine particles may affect the manner of dust removal in some field operations. Therefore, if the average fabric loadings, W, are 200 and 500 g/m^2, respectively, average fabric decelerations, $\bar{a}$, of 250 and 100 g are required to achieve complete surface cleaning. Test results for single and multiple bag experimental units have shown total fabric dust loadings, $W_c + \Delta W$, to range from 400 to 1000 g/m^2 with the greater portion distributed uniformly upon the fabric surface.[5,8] Therefore, any deceleration rate

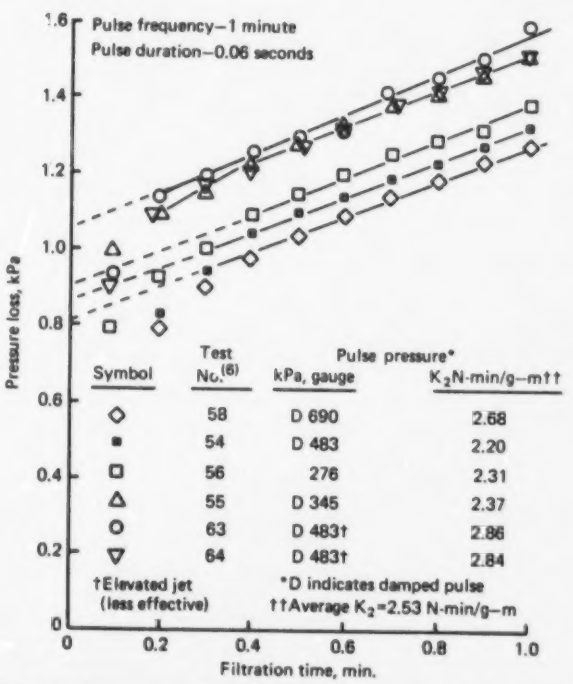

Figure 1. Resistance characteristics and K_2 values for fly ash with Dacron felt, inlet concentration = 27.6 g/m^3, filtration velocity = 2.6 m/min. Linear intercept at time zero is effective residual pressure loss, $(Pe)_{\Delta W}$.

* Pulse damping refers to the process of extending the bag venting time at pulse cessation to reduce dust penetration.[2,8]

exceeding 125 g's would suffice to detach completely the surface layer. Bag *deceleration* is the controlling parameter because it is the rapid slowdown of the dust-laden fabric from its maximum velocity state that produces the tensile stress or separation force, at the dust-fabric interface:

$$F_s = (W_c + \Delta W)\bar{a} \qquad (4)$$

The descriptors for pulsed bag motion, Table I, suggest that operation of a single tube filter at simulated field conditions produces deceleration rates ranging from 225 to 296 g's depending upon the measurement method.[2] In view of the complexity of these measurements, the comparative values for maximum bag displacement from midposition, maximum velocity prior to deceleration, and maximum deceleration show surprisingly good agreement among themselves as well as with the theoretically computed values (Item 5, Table I).

Table I. Experimentally determined descriptors of pulsed bag motion. Dacron (needled) felt bag, 1.22 m long, 11.4 cm diameter.[2]

Measuring procedure	Maximum displacement (cm)	Maximum velocity (cm/s)	Maximum deceleration (g)
1. Static measurements			
Displacement versus pressure	0.66		
2. High speed camera[a,b]			
Fabric	0.84	349	296
Dust		192	
3. Strain gauge[a]	0.61	200	272
4. Accelerometer[a]			225
5. Computed values			
Expansion modulus and pressure/time traces		137[c]	276[d]
6. Dust trajectory		61.0	

[a] Cleaning system—483 kPa (70 psig), 0.06 s pulse (actual time).
[b] Observed frequency—133 cps.
[c] Computed from Eq. 6.
[d] Computed from Eq. 8, see Table II.
Note: Inlet concentration (fly ash) ~25 g/m³, filtration velocity = 2.6 m/min.

One-Dimensional Approximation. During filtration, a typical felt bag drapes inwardly about its supporting cage until the pulse action reverses the pressure differential across it. For the cleaning conditions described in Table I, the fabric undergoes a total radial displacement of approximately 0.7 cm in moving to its fully inflated position. Experimentally determined static displacements for wool and Dacron felt bags are indicated in Figure 2 as a function of pressure differential. At small pressure differentials, little pressure is required to move the bag in either direction to the extent of its slackness since the pressure need only overcome the frictional stiffness of the filter. After the slackness is removed, fabric tensile properties dominate the motion such that further displacement is minimal. In reversing the pressure differential, hysteresis results because of interstitial friction within the fabric. However, since the cleaning process relates to the outward, inflationary motion, only the lower curve for each bag applies.

The continuous curve may be approximated by two linear branches where, for estimating purposes, the G branch describes the slope in the region where bag flexibility or stiffness is controlling and the M_e branch is the region where elasticity or tensile forces prevail. For dust-laden Dacron bags, the comparative values for the G and M_e parameters, 0.054 cm (radial displacement)/cm water pressure and 0.002 cm (elongation)/cm water pressure, respectively, suggest that resistance to flexure controls most of the radial displacement.

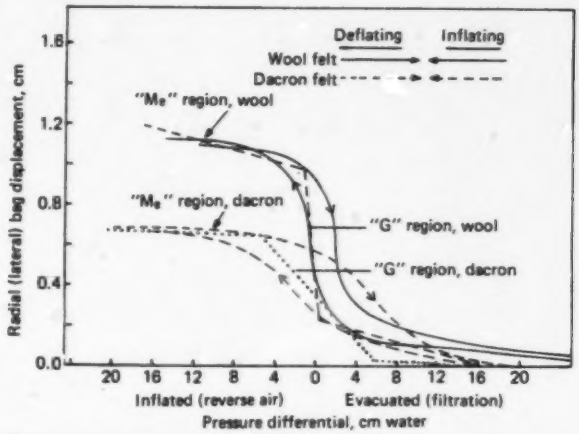

Figure 2. Static displacement of fabric surface at fixed differential pressures with used bags, 1.22 m long × 11.4 cm diameter.

Under these conditions the one-dimensional equation for radial motion can be approximated as follows:[2]

$$\frac{\rho d^2 r}{dt^2} + \frac{r}{G} = \Delta p \qquad (5)$$

where ρ is the mass per unit area for the dust-laden bags, r its radial travel, r/G the resistance force due to bag stiffness, and Δp the instantaneous pressure differential produced by the jet pulse.

Lightweight Fabrics, Motion Controlled by Stiffness. If the bag motion is governed mainly by its stiffness, (or if radial displacement alone without regard to time is the primary concern), Eq. (5) can be approximated by the simpler form, $r/G = \Delta p$. Upon differentiating and rearranging, a useful expression evolves for estimating maximum fabric velocity:

$$dr/dt = V_{max} = Gd(\Delta p)/dt \qquad (6)$$

By assuming linear elastic stretching and negligible friction losses, the bag kinetic energy at midpoint is approximated by the stored elastic energy after the fabric decelerates to its fully expanded state:

$$1/2\rho V_{max}^2 = 1/2M_e(\sigma_{max})^2 \qquad (7)$$

where σ_{max} is defined as the stopping force per unit area, r_{max}/M_e. Since peak deceleration, a_{max}, can be expressed as σ_{max}/ρ, Eq. (6) and (7) may be combined to allow estimation of a_{max} in terms of the following parameters: the density of the dust-laden fabric, ρ; the stretch and flexing moduli for the fabric, M_e and G; and the rate of change of pressure differential across the bag during pulsing, $d\Delta p/dt$.

$$a_{max} = \frac{G}{\sqrt{\rho M_e}} \cdot d(\Delta p)/dt \qquad (8)$$

Eq. (8) provides a means to calculate the separating force, F_s, generated by pulse action in terms of peak fabric deceleration, a_{max}, and the dislodgeable fabric loading, $W_c + \Delta W$.

Table II. Fabric and pressure parameters for estimating maximum deceleration of lightweight, moderately stiff Dacron felt.

Parameter	Numerical value: As measured	Numerical value: cgs units
G	0.054 cm/cm H_2O	5.51×10^{-5} cm² − s²/g
M_e	0.002 cm/cm H_2O	2.04×10^{-6} cm² − s²/g
ρ	0.126 g/cm²	1.26×10^{-1} g/cm²
$d(\Delta p)/dt$	2540 cm H_2O/s	2.49×10^{6} g/cm − s³
a_{max}	(from Eq. 8)	2.71×10^{5} cm/s² or 276 g's

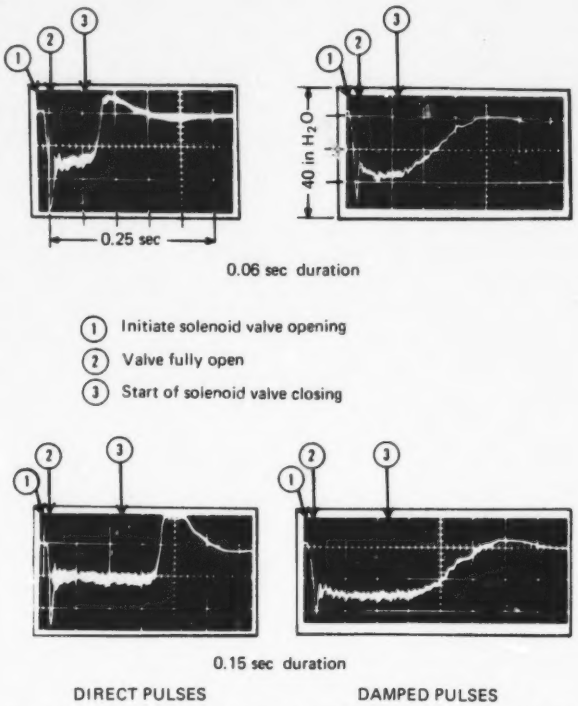

Figure 3. Differential pressure, Dacron bags 4 ft × 4.5 in. (1.22 m × 11.4 cm), fly ash filtration, 1 pulse per minute at 70 psig (483 kPa).

Despite the simplifying assumptions, use of Eq. (8) in conjunction with the operating parameters shown in Table II provided an estimate of deceleration rate, a_{max}, that agreed well with measured values shown in Table I.

Although the terms G, M_e, and ρ are not difficult to determine with a *single* bag experimental system, highly specialized equipment involving oscilloscope displays of pressure transducer outputs are necessary to establish the rate of pressure rise, $d(\Delta p)/dt$, within a bag during the pulse interval. Furthermore, even with a_{max} defined, there still remains the problem of estimating the characteristic cycling dust holding, W_c, for a specific dust-fabric system except by direct weighing or thickness gauge measurements. Therefore, the principal value of Eq. (8) *at this time* is to guide the user in the selection of bag and cleaning parameters.

On the other hand, a strong correlation was demonstrated between the photographically determined $d(\Delta p)/dt$ values, Figure 3, and their corresponding effective residual pressure loss levels $(P_E)_{\Delta W}$, Figure 4. This correlation enabled extension of the modeling capabilities of Eq. (2) and (3) to include the effects of nozzle dimensions, solenoid valve opening times, and bag size for the designated reservoir pressure.

Fabric Media Physical Properties vs. Performance Potential

Eq. (8) indicates that increased flexibility as defined by the parameter, G, causes the fabric to decelerate more rapidly, thereby increasing the magnitude of the dust separating force and the amount of dust removal. Thus, cleaning difficulties may arise if, in attempting to provide a heavier and stronger felt, the penalty of decreased flexibility (or increased stiffness) reduces its initial acceleration capability. Stiffness may also result from dust deposits that increase residual fabric drag, as well as restricting the fabric motion. The increased flexibility for wool felt compared to that for Dacron, Figure 2, may be due to the random dispersion of the fibers in the wool felt. Despite fiber interlockings, the linkages do not favor transmission of localized resistance forces over the length of a bag to the extent possible with the continuous weave of the needled felt scrim. Except for a slightly heavier weight for the Dacron felt, (610 g/m^2 vs. 543 g/m^2 for natural wool) and a small reduction in thickness (0.17 cm vs. 0.20 cm) the properties of both fabrics were essentially the same.

Although highly flexible fabrics are desirable during the *flip-flop* or flow reversal phase of the cleaning motion so that the fabric attains its highest possible velocity, Eq. (8), minimal elasticity or stretching is required to maximize the final deceleration phase. This observation highlights the fact that the desired attributes of high G and low M_e values may sometimes be mutually exclusive. For example, although natural wool felt demonstrates greater flexibility according to Figure 2 it also exhibits a greater elasticity than fabrics from continuous, multifilament yarns. Thus, the initial advantage of a higher velocity during the flow reversal phase (relative to a needled felt) may be offset by a reduction in deceleration due to increased stretch, M_e, properties of a natural wool felt. With extended service life, most fabrics will exhibit a gradual stiffening, which by itself, suggests reduced cleanability. On the other hand, since M_e values may also decrease (roughly 20% for sateen weave cotton and crowfoot weave Dacron),[2] the resulting increase in deceleration during the final stopping phase may partially compensate for the adverse stiffening effect.

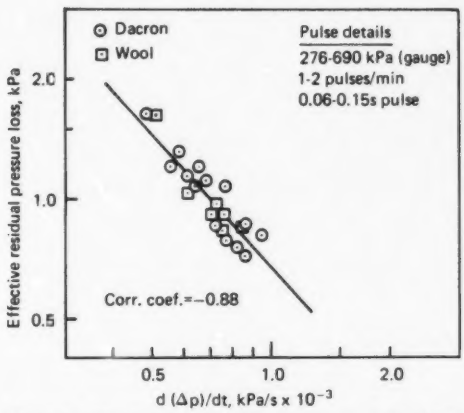

Figure 4. Effective residual pressure loss versus $d(\Delta p)/dt$, 0 to 0.01 s. Fly ash filtration at 2.6 m/min.

Jet Pulse Characteristics

Primary Air Volumes. Jet pulse characteristics were evaluated over a broad range of operating conditions for a single bag system in which needled Dacron or natural wool felts were pulse-cleaned with a conventional commercial nozzle and venturi assembly. Experimental data evaluated here were based on coal fly ash (MMD = 9.2 μm, σ_g = 2.0) filtration at 2.6 m/min with 1.22 m long by 11.4 cm diameter bags, and inlet concentrations in the 20 to 35 g/m^3 range. Pressure regulating valves and pulse durations were adjusted to operate at the reservoir pressure and pulse durations (actual valve open times) indicated in Table III with the option to select pulse frequencies ranging from 0.5 to 2 pulses/min. The primary air volumes for 0.06 and 0.15 s pulses as well as the smaller volume ejected from the nozzle during its 0.01 s opening period are given in Table III. The primary air volume should not be confused with the total volume of air pumped into the bag as a result of jet entrainment of secondary air.

Estimation of $d(\Delta p)/dt$ from Pressure-Time Traces. The oscilloscope traces shown in Figure 3 describe the behavior of short (0.06 s) and long (0.15 s) pulses delivered under normal and damped conditions. As displayed in Figure 3, increasing pressure is read downward as the time scale advances

Table III. Delivered air volume (primary air) vs. reservoir pressure, direct pulses.

Reservoir pressure gauge		Measured primary air volume[a] per pulse, $m^3 \times 10^3$, STP		
		Valve opening period	Total pulse duration	
kPa	psi	0.01 s[b]	0.06 s	0.15 s
276	40	0.28	3.0	6.0
483	70	0.48	5.4	10.5
621	90	0.68	7.4	13.9
690	100	0.77	8.5	16.2

[a] Air from several pulses collected in sounding balloon and transferred to spirometer for metering.
[b] Volume assumed to be half that delivered in subsequent full-open 0.01 s periods.
Note: Standard pulse jet, nominal ¼-in. nozzle (actually 0.363 in diameter) and timing controls, Mikro-Pul Division, U.S. Filter Corp., Summit, N.J.

from left to right. Their form follows closely the structure observed previously by Bakke,[6] and Dennis and Silverman[1] who also used sensitive pressure transducers for tracking rapid pressure changes. The latter measurements[1] also showed that the pressure gradients determined at mid bag length were a good representation of conditions over the whole bag. Pressure differentials increase rapidly at first because venting of the pulse air is restricted by the overlying dust layer. It appears that most dust releases when or just before the solenoid valve is full-open because the pressure decreases suddenly after the first 0.01 s to a lower level that remains nearly constant until the valve is shut. The normal pressure reduction rate is roughly the same as that for the inflation period, whereas a very gradual return results with pulse damping. It was observed that the initial slopes, $d(\Delta p)/dt$, of the pressure-time traces correlated well with the previously discussed *effective residual pressure*, $(P_E)_{\Delta W}$, as shown in Figure 4, viz;

$$(P_E)_{\Delta W} = 1600(d(\Delta p)/dt)^{-1.13} \tag{9}$$

Effect of Cleaning Parameters on $d(\Delta p)/dt$. Eq. (9) has no predictive value unless $d(\Delta p)/dt$ can be redefined in terms of readily determined design and operating parameters characterizing the filter system of interest. An analysis of the pulse jet cleaning process suggests that four major variables govern the rate of pressure rise in a pulsed bag: the absolute reservoir pressure, P_{ja}; the cross sectional area of the delivery nozzle, A_j; the opening time for the solenoid valve, t_s; and the volume of the bag itself, V_b. Experimental data, Table IV, also indicates that $(P_E)_{\Delta W}$ is an approximate linear function of both P_{ja} and the maximum static pressure observed on the clean air side of the bag, P_{max}; i.e.,

$$d(\Delta p)/dt \propto (P_{ja}) \propto (P_{max}) \tag{10}$$

The volume of primary air, V_p, delivered during the solenoid valve opening period can be estimated by the following expression.

$$V_p = (M/\rho_b)(t_s/2) \tag{11}$$

where M is the nozzle mass flow rate, ρ_b the primary air density reduced to bag conditions, and $t_s/2$ is the *effective* opening time for the solenoid valve. It was assumed that the *effective* mass flow rate, M, during the opening interval was roughly half that of the full-open state. Because the ratios of reservoir, P_{ja}, to bag pressure before cleaning, P_b, usually exceed the critical level, r_c, of 0.53 where acoustic velocities obtain, i.e. $P_{ja}/P_b > 1/0.53$, where P_b refers to the bag static pressure before pulsing, mass flow can be calculated by the compressible flow relationship[9]

$$M = 40.4C_v P_{ja} A_j/\sqrt{T_{ja}} \text{ (metric units)} \tag{12}$$

in which C_v is the coefficient of velocity (dimensionless and assumed to be unity) P_{ja} the compressed air reservoir pressure in kPa, A_j the jet nozzle cross section in m^2, and T_{ja} the reservoir air temperature in °K, where the subscript a designates absolute values for compressed air temperature and pressure.

Although the combined action of the jet nozzle and the venturi element at the bag exit has been correctly described as a jet pump system,[6] the analysis of its performance during the initiation of the pulse places the entire entrainment process in the nonsteady state realm. Hence, the classical, semi-empirical relationships between pressure ratios and the ratios for primary and secondary air flow rates do not apply. For estimating purposes, it was assumed that during the solenoid valve opening time of 0.01 s, primary and secondary air were ejected into the bag with no permeation through the dust-laden bag and no reverse (180°) venting from the bag.

The average pressure observed within the bag during the inflation process reflects the air volume contributed by the primary flow plus the secondary volume, V_s, resulting from momentum transfer to the surrounding air from the sonic velocity jet. At the completion of the filling process, assuming that no air has vented from the bag, the instantaneous bag pressure will have been increased from its original base level during filtration, P_B, by the factor $(V_p + V_s)/(V_b + V_p + V_s)$. When the bag volume far exceeds the air volume injected by the pulse, the rate of pressure increase $d(\Delta p)/dt$ may be defined by the approximate expression

$$d(\Delta p)/dt = \left(\frac{V_p + V_s}{V_b}\right)\left(\frac{P_b}{t_s}\right) \tag{13}$$

Although V_s is not readily determined, it may be inferred from Eq. 11 through 13 that $(V_p + V_s)$ should also be directly proportional to V_p; i.e., $V_p + V_s = kV_p$. Strictly speaking, Eq. (13) describes the rate of pressure increase on the downstream (clean) side of the bag and not the pressure differential across the bag that causes the bag motion. However, because dirty side pressures are ordinarily very small compared to their clean side counterparts, Eq. (13) constitutes a good approximation of $d(\Delta p)/dt$ as may be inferred from Eq. (10).

By combining and rearranging Eq. (11) through (13), $d(\Delta p)/dt$ can be expressed as follows:

$$d(\Delta p)/dt = (k20.2P_{ja}A_j/\sqrt{T_{ja}})(P_b/V_b\rho_b) \tag{14}$$

where P_b is the absolute pressure on the clean side of the bag in kPa, V_b the bag volume in m^3, and ρ_b the ambient (bag) air density in kg/m^3. A value of 2.12 was computed for the constant k, based upon the data presented in Table IV and the physical units used in Eq. (14). If filtration is performed at sea

Table IV. Variation of maximum cleanside bag pressure and $d(\Delta p)/dt$ with reservoir pressure. Fly ash filtration at 2.6 m/min, 1.22 m × 11.4 cm bag.

Reservoir pressure			$d(\Delta p)/dt$ kPa/s		Maximum clean-side bag pressure kPa	
Absolute	Gauge					
kPa	kPa	psig	Dacron[a]	Wool[a]	Dacron[a]	Wool[a]
377	276	40	527 ± 72	503 ± 70	7.28 ± 0.85	8.97 ± 0.94
584	483	70	680 ± 82	723 ± 84	9.12 ± 0.94	9.90 ± 0.98
794	693	100	925 ± 95	922 ± 95	13.5 ± 1.14	12.5 ± 1.11

[a] Estimated means and standard deviations.

level conditions where values of 21.1°C, 101.6 kPa, and 1.2 kg/m^3 may be assumed for T_{ja}, P_b, and ρ_b, respectively, Eq. (14) may be reduced to the simple form

$$d(\Delta p)/dt = 211 P_{ja} A_j / V_b \quad (15)$$

Summary and Conclusions

Theory and experiment indicate that total bag mass, tensile properties, and flexibility influence the rate at which the bag is accelerated and decelerated by the pulse action. Maximum deceleration, which plays an important role in pulse jet filter systems, can be computed as shown below:

$$a_{max} = \frac{G}{\sqrt{\rho M_e}} \cdot d(\Delta p)/dt \quad (8)$$

Although the variables appearing in Eq. (8) are difficult to measure except in the laboratory, the fact that the rate of pressure increase within a bag, $d(\Delta p)/dt$, can be predicted in terms of readily defined design and operating parameters, Eq. (14) and (15), provides the basis for a useful set of working equations. By successive substitutions of the semi-empirical relationships for $d(\Delta p)/dt$ and $(P_E)_{\Delta W}$

$$d(\Delta p)/dt = 211 P_{ja} A_j / V_b \quad (15)$$

$$(P_E)_{\Delta W} = 1600[d(\Delta p)/dt)]^{-1.13} \quad (9)$$

the pressure loss for a single bag pulse jet filter can be predicted by Eq. (2) when the variables in the last term are known.

$$P = (P_E)_{\Delta W} + 0.001 C K_2 V^2 \Delta t \quad (2)$$

Given only *one* pressure loss vs. time (or fabric loading) curve such as those shown in Figure 1, the filter designer or user can estimate bag pressure loss for any set of operating conditions that may include variations in inlet dust concentration, filtration velocity, frequency of cleaning, intensity of cleaning as defined by reservoir compressed air pressure, compressed air orifice dimensions and valve opening time, bag volume, and the temperature, barometric pressure, and density of the filtered air. All predictions, however, apply only to the dust-fabric combination described in the single test.

If no data such as given in Figure 1 are available, the predictive equations are only useful when the dust-fabric combination of interest possesses the approximate dust dislodgement or adhesive properties of the coal fly ash-Dacron felt system used to develop Figure 1 and Eq. (9). For example, prior measurements with a more readily dislodged talc dust have shown that the constant, 1600, Eq. (9) should reduce to approximately 630.[2,8] Thus, estimates of effective residual pressure levels would err on the high side by about 0.5 kPa (2 in water) if fly ash data were applied.

The modeling equations described above may be extended to typical multibag, sequentially pulsed field units by iteration processes similar to those used with reverse air or mechanically shaken systems.[10,11]

$$\overline{S} = \left(\sum_{i=1}^{n_b} \frac{a_i}{S_i} \right)^{-1} A \quad (16)$$

where $\overline{S}$ is the average system drag, n_b is the total number of bags, A is the total cloth area, $a_i = A/n_b$ and S_i ranges from $S = (P_E)_{\Delta W}/V$ to $(P_E)_{\Delta W}/V + CK_2V\Delta t$.

A rough estimate of average system drag for a multibag system is also obtained by introducing the coefficient 0.75 into the right hand member of Eq. (2). The latter term designates the drag increase attributable to the freshly deposited loading; i.e., $0.75\, CK_2V\Delta t$.

Acknowledgments

The developments reported in this paper are based in part upon federally funded programs of the Environmental Protection Agency performed under contract number 68-02-0268 and 68-02-1438, Task No. 5. This paper does not necessarily reflect the views or policies of the U.S. Environmental Protection Agency, nor does mention of trade names, commercial products, or organizations imply endorsement by the U.S. Government.

References

1. R. Dennis, L. Silverman, "Fabric filter cleaning by intermittent reverse air pulse," *ASHRAE J.* **4**(3):43 (March 1962).
2. R. Dennis, J. E. Wilder, "Fabric Filter Cleaning Studies," EPA-650/2-75-009 (NTIS No. PB-240-372) Jan. 1975.
3. D. H. Leith, M. W. First, H. Feldman, "Performance of a pulse-jet filter at high filtration velocity—II. Filter cake redeposition," *JAPCA* **27**:636 (1977).
4. M. J. Ellenbecker, D. H. Leith, "Dust deposit profiles in a high velocity pulse-jet filter," *JAPCA* **29**:1236 (1979).
5. M. J. Ellenbecker, D. H. Leith, "Theory for dust deposit retention in a pulse-jet fabric filter," *Filtr. and Separation* **16**(6):624 (Nov./Dec. 1979).
6. E. Bakke, "Optimizing filtration parameters," *JAPCA* **24**:1150 (1974).
7. L. R. Lefkowitz, "Evaluation of Felted Glass Media under Simulated Pulse Jet Operating Conditions," In *Symposium on the Transfer and Utilization of Particulate Control Technology: Volume 4, Fugitive Dusts and Sampling, Analysis and Characterization of Aerosols*, EPA-600/7-79-044b (NTIS No. PB-295-229) Feb. 1979.
8. R. Dennis, H. A. Klemm, "Modeling concepts for pulse jet filtration," *JAPCA* **30**:38 (1980).
9. D. F. Boucher, G. E. Alves, "Fluid and Particle Mechanics," in Perry's *Chemical Engineers Handbook*, 4th Ed., McGraw-Hill Book Company, Inc., New York, 1963 p 5–9, 5–10.
10. R. Dennis, H. A. Klemm, "A model for coal fly ash filtration," *JAPCA* **29**:230 (1979).
11. R. Dennis, R. W. Cass, R. R. Hall, "Dust dislodgement from woven fabrics versus filter performance," *JAPCA* **28**:47 (1978).

Mr. Dennis is a member of the Environmental Engineering Department of GCA/Technology Division, Bedford, MA 01730. Dr. Wilder is associated with S. D. Warren, A Division of the Scott Paper Company, Westbrook, ME 04092. Mr. Harmon is a member of the Industrial Environmental Research Laboratory, U.S. Environmental Protection Agency, Research Triangle Park, NC 27711.